

Contents lists available at ScienceDirect

Petroleum Science

journal homepage: www.keaipublishing.com/en/journals/petroleum-science



Original Paper

Reservoir characteristics of Datta Formation (Early Jurassic), Marwat-Khisor Ranges, sub-Himalayas, Pakistan



Muhammad Tariq ^a, Muhammad Kashif ^{a, *}, Noor Ahmed ^a, Zaheen Ullah ^b, Jose Nicanor Mendez ^c, Muhammad Armaghan Faisal Miraj ^d

- ^a Department of Earth Sciences, University of Sargodha, Sargodha, 40100, Pakistan
- ^b Department of Geosciences, University of Baltistan, Skardu, Pakistan
- ^c School of Geosciences, China University of Petroleum, Qingdao, 266580, China
- ^d Institute of Geology, University of the Punjab, Lahore, Pakistan

ARTICLE INFO

Article history:
Received 10 March 2022
Received in revised form
27 March 2023
Accepted 13 April 2023
Available online 14 April 2023

Edited by Jie Hao and Teng Zhu

Keywords: Reservoir characteristics Jurassic Datta Formation Porosity. permeability Sandstone

ABSTRACT

The present work has been accomplished to carry out a detailed study of the characteristics of the Early Jurassic Datta Formation of Trans-Indus Ranges, Pakistan. The discovery of Saib well-1 (Gas and condensate discovery from Jurassic limestone) in the study basin takes an active interest in carrying out extensive exploration activities in the same basin. Jurassic rocks especially Datta Sandstone and Samana Suk Limestone are acting as good reservoirs. The study unit consists of variegated sandstone interbedded with siltstone, carbonaceous clay, and shale and coal stringer. For the current work, two stratigraphic sections (Pezu and Abbo Wanda) have been measured. To examine its sedimentology, depositional environment, diagenetic settings, and reservoir characteristics, a detailed study was conducted and various laboratory techniques have been utilized. About 95 rock samples from the bottom to the top of both sections were collected, and 50 rock samples have been selected for thin section analysis and were examined under a polarizing microscope to show their mineralogical composition, diagenesis, and their reservoir characteristics. XRD (X-ray diffraction), Cathodoluminescence (CL), SEM (Scanning electron microscope) with EDS (Energy-dispersive spectroscope), and Core plug porosity and permeability analysis have been used to interpret its chemical and mineralogical composition and its reservoir characteristics, respectively. Based on field observations and thin section analysis, four depositional facies and six lithofacies have been established. The sedimentary structures, depositional facies, and lithofacies indicate that Datta Formation was deposited in a deltaic environment, Compactions, cementation, fracturing and dissolution can greatly affect the quality of reservoir rock. Based on thin section and SEM analysis, large numbers of primary pores, fracture and secondary pores were observed and connectivity between the pores is good, and at some places, these pores were filled through the authigenic clay minerals like kaolinite, mixed layers illite/smectite and chlorite that influences the reservoir characteristics. Primary pores (thin section) and secondary pores (dissolution pores) and core plug porosity and permeability data (porosity 13.23%-26.89% and permeability 0.12 to 149 mD) shows that Datta Formation has a good reservoir quality.

© 2023 The Authors. Publishing services by Elsevier B.V. on behalf of KeAi Communications Co. Ltd. This is an open access article under the CC BY-NC-ND license (http://creativecommons.org/licenses/by-nc-nd/4.0/).

1. Introduction

Marwat-Khisor Range is the part of Trans Indus Ranges. During the collision between the Indian and Eurasian Plates, this range has been formed as a result of continuous southward decollement The Foreland Fold-and-Thrust Belt of northwestern Himalayans was signified by the western portion of these Ranges. The Marwat-Khisor Range is located in the central part of the Trans-Indus Ranges, delineating a northeast-southwest trending Fold-Thrust Belt system to east-west (Khan et al., 2013). The boundaries of the Marwat-Khisor Range do not prevent any commercial discovery, although in 1866, in the subcontinent, the first exploration well

associated thrusting of the sedimentary Shield of the Indian Plate.

E-mail address: kashifyaqub@yahoo.com (M. Kashif).

^{*} Corresponding author.

(Kundal-1) was drilled in this region located at the foot of Khisor Range (Khan et al., 2013). A significant quantity of commercial oil and gas was produced mostly from carbonate rocks (Bosence et al., 1996). The sedimentary units have major significance as hydrocarbon reservoirs that are deposited and filled up the basin during the Jurassic age (Brannin et al., 1999).

In the study area, the Jurassic rocks are the primary hydrocarbon reservoir rocks (Csato et al., 2001). Accumulated oil for commercial use of the Jurassic clastic rock, where huge amounts of oil were extracted by drilling from numerous wells. The accumulated oil of Jurassic rocks is mostly comprised of an organic substance derived from the marine environment (Hakimi et al., 2012). Reservoir characterization is used to determine the porosity, permeability, net-to-gross, water saturation, and pore fluid of the reservoir. One of the main sources of energy nowadays is hydrocarbon and its product linked to it. Pakistan is struggling to explore its hydrocarbon resources with many commercial and non-commercial initiations. Though, the maximum of the shallow clastic reservoir of Jurassic rocks with a high water cut reached the depletion phase (Brannin et al., 1999). In Toot, Meyal, and Dhulian oil fields in the Upper Indus Basin, Datta Formation is producing thickly exposed beds in Sheikh Badin Hills in the Marwat Range. The clean and quartos beds of sandstone and the delta front facies allow very good reservoir characteristics (Zaidi et al., 2013). The current study area was poorly explored leading to several doubts which delayed further exploration and development strategies. The relation between the diagenesis and depositional facies is critical for envisaging the dispersal of diverse diagenetic aspects which sturdily regulate the facies reservoir quality. The study of reservoir characteristics in the Marwat-Khisor ranges is a significant contribution to oil and gas exploration.

Geochemical records conducted by good samples (OGDCL and HDIP) signify the sufficient quantity of organic matter that has been found in Datta Formations. The present study was undertaken to carry out a detailed sedimentological study and reservoir characteristics of the Datta Formation. The challenges and perspectives for future developments in reservoir characterization are also discussed. The main objectives of the current study are: 1) to evaluate the diagenetic features based on thin section and SEM analysis, and 2) to evaluate the reservoir characteristics based on core plug porosity and permeability analysis.

2. Regional geology

The Trans-Indus Ranges are a western expansion of the Salt Range across the Indus River and are represented by the small dissected mountains at the southern periphery of the Sub Himalayas (Fig. 1) (Gee, 1989). These ranges mark the southernmost deformational front of the Himalayan orogeny with the undeformed sediments of the Punjab Platform (Hemphill and Kidwai, 1973). Sheikh Badin Hill, the southernmost terminal of NS trending Marwat Range is characterized by the doubly plunging fold cutting by three thrusts Pezu Fault, Sheikh Badin Fault, and Paniala Fault (Kazmi and Rana, 1982). Sheikh Badin Hill crops out the sedimentary sequence ranging from Late Permian to Pliocene-Pleistocene with three major unconformities (Fatmi and Kennedy, 1999).

The central part of the Trans-Indus Ranges is comprised of the Marwat-Khisor Range where these ranges turn to the southeastern boundary of Bannu Basin. Asymmetric, south-verging overturned and plunging fold structures along with related thrust faults derived from the basal decollement represent the structural style of the Marwat-Khisor Ranges. The tectonic history of Sheikh Badin Hills and Khisor Ranges has been comprised with two distinct events of Late Cenozoic tectonism including early normal faulting

in the basement followed by south verging thrusting of sedimentary succession on the top of the basal decollement (Blisniuk et al., 1998). Khisor Range has been tectonically uplifted and distorted due to the youngest active Khisor Frontal Thrust. Structural investigation of the study area recommends that the environment of deformation is thin-skinned containing assemblages of thrust-fold, associated with local basal decollement positioned at the bottom of rocks of the lhelum group (Alam, 2008).

The stratigraphic succession exposed in both Pezu and Abbo Wanda section of Sheikh Badin Hills, Marwat-Khisor Ranges consisting of Jurassic to Pliocene rocks (Fig. 2). With contrasting Khisor Range, the Jurassic rock, i.e., Datta Formation, Shinawari Formation and Samana Suk Formations underlay the Triassic rocks in Sheikh Badin Hills, and the Jurassic rocks are underlain by Cretaceous rocks of Chichali and Lumshiwal Formations. The Datta Formation consists of mainly variegated colored sandstone, with subordinate siltstone and mudstone, and shale (Fig. 3a). The sandstone is fine to coarse-grained, thick or thin-bedded, soft, friable, and micaceous in places. Calcareous shale is present close to the top of the formation, carbonaceous shale in the middle part, and gypsiferous shale close to the bottom of the formation. Silica sand is a unique feature of the basal part of the formation.

The Shinawari Formation contains grey, thin to medium beds of sandy limestone along with calcareous sandstone with minute interbedded shale (Fig. 3b). The Samana Suk Limestone is brown and grey crystalline and fine grain thin to thick-bedded oolitic limestone that is argillaceous in the region (Fig. 3c and d) with chop board weathering. The Chichali Formation consists of glauconitic sandstone in the upper part of the formation that is brown and grey, soft, and friable (Fig. 3d) with subordinate blue-grey shales that are thin-bedded and silty. Dark-grey siltstones in the lower part are glauconitic and calcareous shale, and the lowest bed contains belemnites. The Lumshiwal Formation consists of grey color mudstone beds and fine to medium grain ferruginous sandstone with glauconitic sandstone and intermittently belemnites in Sheikh Badin Hills. The Nagri Formation consists of grey sandstone that commonly weathers brown and crops out in zones 20-60 feet thick. The Dhok Pathan Formation consists of brown claystone and a subsidiary quantity of brown sandstone showing hematic alteration.

3. Methodology

Two well-exposed sections (Pezu 88 m thick and Abbo Wanda 103 m thick) in the Marwat-Khisor Ranges were selected for detailed investigation based on the standard principle of sedimentology and reservoir characteristics. About 95 rock samples have been collected from two studied sections (50 samples from Abbo Wanda and 45 samples from Pezu section), from which 50 rock samples (28 from Abbo Wand and 22 from Pezu section) have been selected for thin sections analysis (Fig. 4). Rock grains, their size, shape, orientation, deformation, contact nature, cement, and other diagenetic features have been observed under a polarizing microscope and SEM. The micro photo was taken with an attached digital camera (Optical-B9) using a compound microscope (Lambomed, CXR3) and a Pentium IV Computers with achromatic capabilities of X4, X10, and X40 magnification at the Department of Earth Sciences, University of Sargodha. SEM with EDS analyzes the diagenetic minerals, pores, and chemical properties of a specimen. Selected samples (10) were subjected to SEM with EDS analysis with specification JSM5910/INCA200, Oxford instruments U.K, at Central Resource Laboratory (CRL), University of Peshawar.

To identify clay minerals and other minerals composition with the exact mineral phase, XRD has been performed. XRD is a powerfilled PC program that identifies the number on each position and

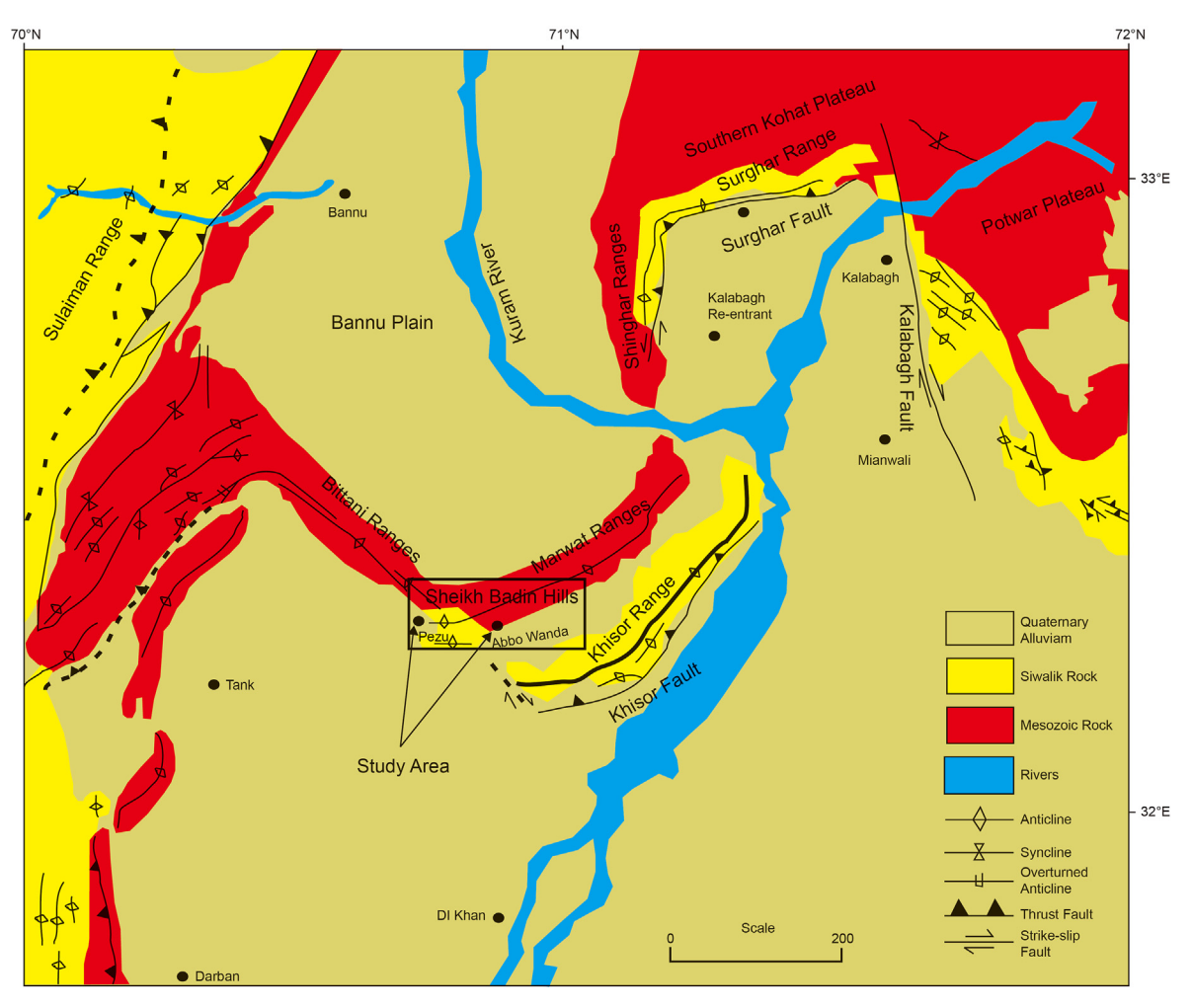


Fig. 1. The geological map of the study area (modified after Yaseen et al., 2021).

then compares it to the specific pinnacle number in the pinnacle chart. It gives the properties of theta (θ) and the counts/second. Selected samples were sorted according to standard methods (Tucker, 1988) and subjected to XRD examination with specifications JDX-3532, JEOL, JAPAN at Central Resource Laboratory (CRL), University of Peshawar.

Cathodoluminescence (CL) analysis has been used to identify the stages of carbonate cement by using a microscope. Selected samples (10) have been subjected to cathodoluminescence (CL) with a specification Zeiss AxioCam 506 color, instrument at the Central Resource Laboratory (CRL), University of Peshawar. The core plug porosity and permeability of sandstone, and splintered cores (Fig. 5) have been calculated under ascetic stress circumstances. To calculate the reservoir characteristics of sandstone and fractured cores, the core plug porosity method has been used. These procedures were performed at the Hydrocarbon Development Institute, Islamabad, Pakistan.

4. Results

4.1. Lithofacies

A detailed study indicates that Datta Formation is extremely diverse and structurally immature to somewhat mature, and sedimentation manages the primary porosity and influences the postmodification process to a definite degree as anticipated by

Hammer et al. (2010). Lithofacies are assessed through physical properties, e.g. grain size, the existence of the rock fragments, fossil remains, and arrangement of grain, and their distinctive lithofacies have been identified. These are described below.

4.1.1. Conglomeratic sandstone

This lithofacies is mainly comprised of sandstone with a conglomerate of different sizes with a few trough cross-bedding, graded bedding, and ripple marks. Moderately sorted sub-angular to angular grains with well-distributed intergranular porosity, and good connectivity pores are present. Based on petrographic observation, present facies comprises mixed pebble, gravel, mud, and sand. Sub-angular feldspar and quartz are the main component of sandstone and have been deposited in-stream channels, and the alluvial fan environment. These facies comprise 8% of all lithofacies in both sections.

4.1.2. Coarse-grain sandstone

In this lithofacies, the particles are mainly detrital quartz, feld-spar, and lithic rock fragments. Graded bedding is common and has been deposited in a lacustrine and channel environment. These lithofacies have high intergranular primary porosity (max 25%) and secondary porosity (max 5.5%), and have good pore connectivity. It also consists of mixed coarse and medium grain sediment having somewhat lower porosity comparable to conglomeratic sandstone (Fig. 6). The prevailing cement is calcite with minor quartz

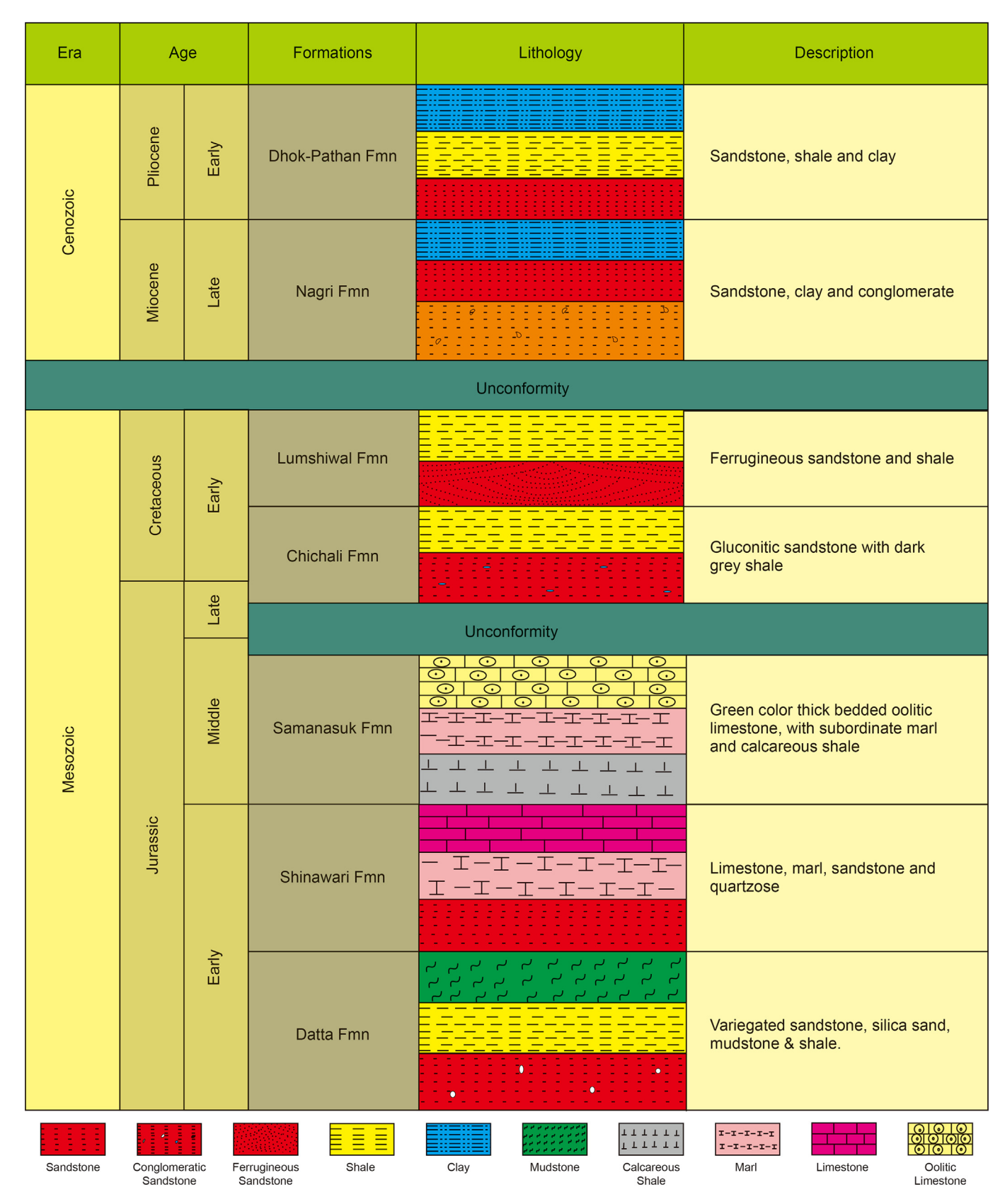


Fig. 2. The stratigraphic succession of Pezu and Abbo Wanda sections, Sheikh Badin Hills, Marwat Range, Trans-Indus Ranges, Pakistan (after Hemphill and Kidwai, 1973).

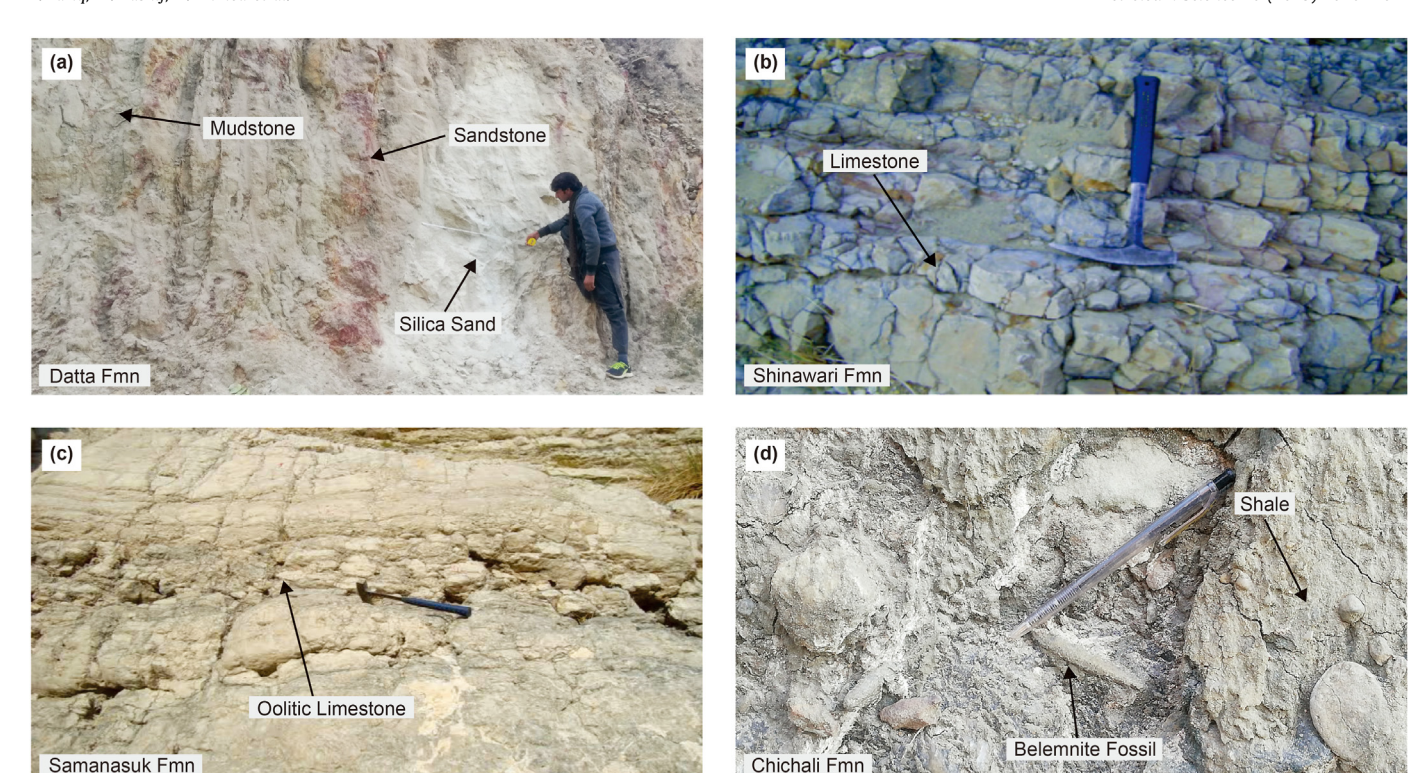


Fig. 3. Field photographs show stratigraphic units of the study area. (a) Represent the Datta Formation comprised of shale, mudstone, silica sand, and sandstone beds. (b) Represent the Shinawari Formation comprised of main limestone. (c) Represent the oolitic limestone of Samansuk Formation (oolitic limestone). (d) Represent the belemnite bearing shale (Chichali Formation).

overgrowth and hematite. These facies comprise 27% of all lithofacies in both sections.

4.1.3. Medium-grain sandstone

Medium-grained sandstone facies mainly consisting of quartz followed by feldspar and rock fragments (Fig. 6). Poorly sorted, subround to sub-angular grains are present with high primary (intergranular) porosity (max 22%) and secondary porosity (max 4.0%). Calcite acts as abundant cement and in some places, the pores were filled through ferrocalcite. The prevailing cement is calcite with minor quartz overgrowth. This type of lithofacies is developed as a channel deposit and in a lacustrine environment. These facies comprise 35% of all litho-facies in both sections.

4.1.4. Fine-grain sandstone

Fine-grain sandstone consists of moderately sorted and subrounded fine-grained sandstone (Fig. 6). Feldspar, quartz, and fragments of lithic rock (Chert, volcanic, and metamorphic rock) are the main constituent of fine sandstone. The present lithofacies usually have an intermediate porosity, and at several places, the dissolution of unstable rock fragments and feldspar grain generates secondary porosity. Point bar elements and fine-grain sandstone are reliable with a meandering river system (Miall, 2013). The current facies comprise 15% of all litho-facies in both sections.

4.1.5. Siltstone

Siltstone and fine-grained sandstone with a large number of mudstone layers are the main constituents of this lithofacies (Fig. 6). Petrographic analysis suggests that sandstone represents inter-laminations of muddy and silty beds. This lithofacies consists of poor to moderately sorted grains and the grains are rounded, angular to sub-angular containing calcite and dolomite content in

muddy layers. The present lithofacies exhibits intermediate to low intergranular porosity, while muddy layers containing microfractures influence the rock permeability. These facies comprise 8% of all litho-facies in both sections.

4.1.6. Mudstone/shale

These facies largely consist of mudstone and shale. Laminated, grey to dark grey color mudstone, and splintery shale is present with a minute amount of siltstone (Fig. 6). This lithofacies is mostly comprised of mudstone and shale, and mostly formed during HST and TST with various fossil shells and mud clasts. Parallel laminated shale shows that the sediments were deposited in a flood-plain setting with a diverse energy state. These facies comprise 7% of all litho-facies in both sections.

4.2. Sandstone composition

Thin section analysis shows that the sandstone in the studied samples mainly falls (Pettijohn et al., 2012) in feldspathic litharenite, lithic Arkosic, followed by Arkosic sandstone (Fig. 7; Table 1). Quartz is the major constituent in studied samples ranging from 40% to 75% (average of 40%); feldspar content ranges from 10% to 55.6% (average of 30.5%); and the rock fragments content ranges from 5.2% to 50.1% (average of 28.4%). The main types of rock fragments were metamorphic rock clasts (fragments), followed by igneous rock clasts (fragments), and a low volume of sedimentary rock clasts. The main contact between the grains is point contact, followed by line contact and concave-convex contact. The sorting property of rocks mainly ranges from medium to poor, and the roundness is mainly subangular, followed by subangular to subrounded. Texturally, the rock unit is not mature but a large number of quartz grains made them mineralogically mature. Pore spaces

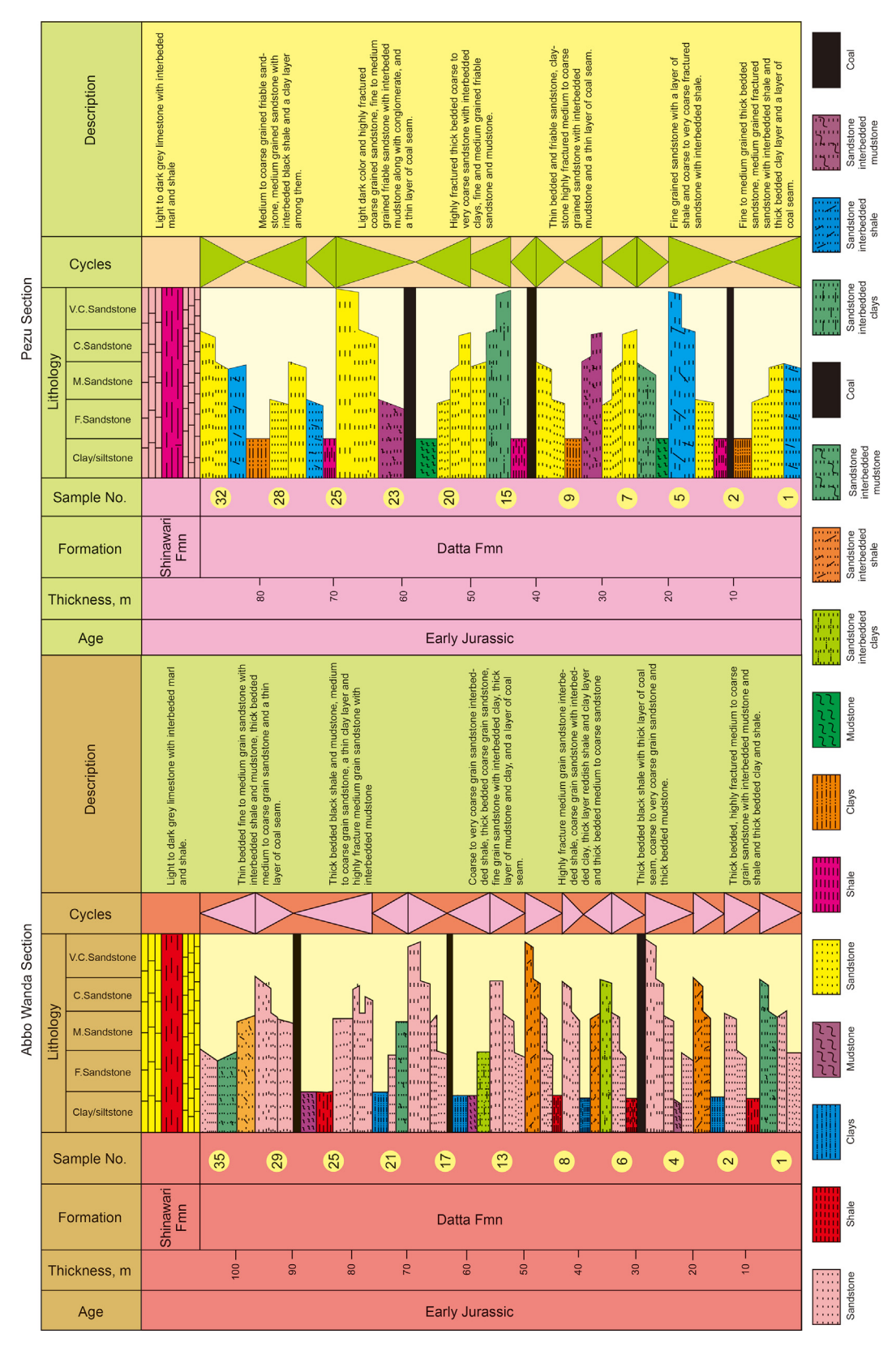


Fig. 4. Litholog of Abbo Wanda and Pezu section with representative selected samples for experimental work.

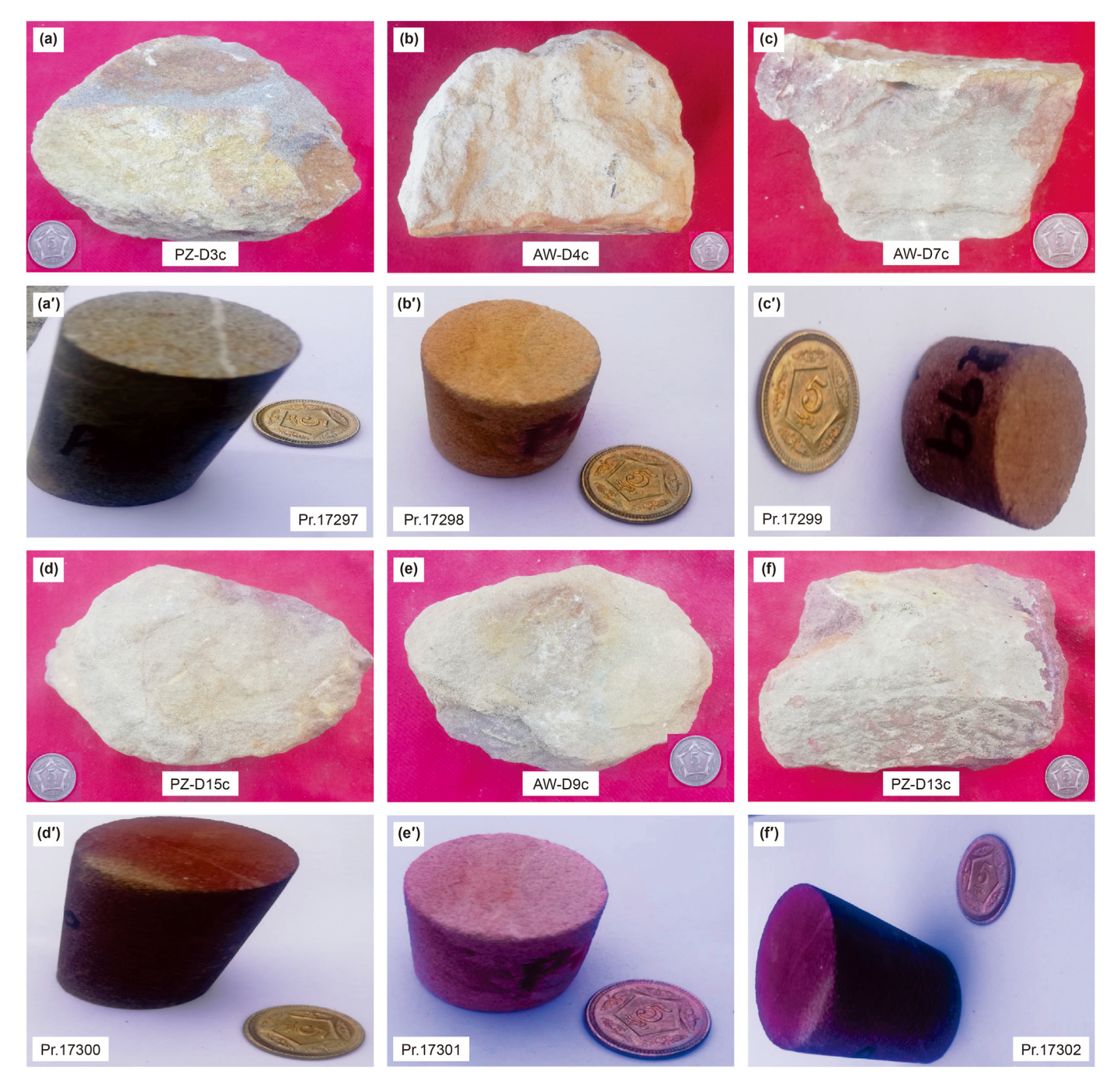


Fig. 5. Photographs show selected field samples and core plug samples studied sections of Datta Formation; (a, d, and f) are field samples, and (a', d' and f') are core plug samples of Pezu section; (b, c, and e) are field samples and (b', c', and e') are core plug samples of Abbo Wanda section.

are blocked by authigenic clays and quartz cement (Fig. 8; Fig. 9). The calcite and hematite cement is seen among the clastic grains. Primary, secondary, and fractured pores were also present in the studied samples (Fig. 9).

4.3. Pore spaces

Thin section analysis shows that both primary and secondary dissolution and fracture pores are present in the studied samples (Fig. 9). These secondary dissolution pores are typically generated, when different types of acidic solution react with the unstable grains and cement, as a result of which the unstable grains

dissolved completely or partly due to their low resistance to the acidic solution (Fig. 8f, g, h; Fig. 9d-h). About 45%–50% of the total reservoir porosity is intergranular primary porosity. About 25% of the remaining 50% is secondary dissolution porosity and the remaining 25% of the 50% consist of fracture pores and cement dissolution pores.

4.4. Pore types, pores shapes, and pore throat characteristics

The studied sandstone consists of good porosity and permeability (Table 2). The results of casting thin section and SEM show that there are two main types of pores (primary and secondary)

Lithofacies	Description	Environment of deposition	Sample photograph
Conglomeratic Sandstone	Consisting of sand supporting conglomeratic sand grains, and the grains are sub-angular and poorly sorted	Base of high-density turbidites, beach and shore of river and lakes.	PZ-D10
Coarse-grain Sandstone	Consisting of coarse grain sandstone, grains are mostly detrital quartz, feldspar and rock fragments	Channel deposit	AW-D4
Medium grain Sandstone	Consisting of medium grain sandstone and mostly consisting of quartz followed by feldspar and rock fragments, grains are poorly sorted and sub-angular to sub-round	Channel deposit	PZ-D15
Fine grain Sandstone	Consisting of fine grain sand, grains are sub rounded and moderately sorted	Developed at the base of low- density turbidites	AW-D9
Siltstone	Consisting of fine grain sandstone with abundant mudstone laminates, siltstone containing much clay	Marginal setting away from the sand input	AW-D6
Mudstone/Shale	Consisting of laminated grey, dark grey mudstone, and shales	Deeper basin with low hydrody- namic force	AW-D21

Fig. 6. The lithofacies, description, and depositional environment along with sample photographs of the Datta Formation.

followed by fracture pores and a small amount of residual intergranular pores. The prevailing pores are the intergranular primary pores (Fig. 9a, b, c, g, h). Grain alignment and brittle and ductile grain deformation are micro-scale mechanical processes that manage to decrease primary pores during compaction (Chester et al., 2004) (Fig. 8a, c). The secondary intragranular pores mainly occurred in the interior of feldspar or debris with irregular shapes (Fig. 9b, d, e, g, h). Fractures are mainly caused by compaction and various tectonic stresses, which are beneficial to acidic or alkaline fluids permeating into particles, causing the dissolution of particles and the formation of fracture pores (Fig. 9a, f, h).

As a bridge between pores, the shape and size of the throat play an influential role in fluid migration and permeability in the reservoir. Three types of pores have been identified i.e, (a) Necking throat: a part of the shrinkage part between the particles due to the close contact of the particles due to compaction, which features a pore radius larger than the throat radius. (Fig. 9b); (b) Flake throat:

mostly found in sandstone with linear or concave-convex contact (Yu et al., 2018). It features small pores and a fine throat, and is also common in the study area (Fig. 9c); (c) Curved flake throat: small, curved, and rough, and is easily blocked (Fig. 9a-c) (Li et al., 2021). Whereas, the shapes of pores are triangular, curved, and tube-like with narrow pore throats (Fig. 9a-c).

4.5. Diagenesis

Digenesis may decrease/increase or preserve the porosity and permeability of sandstone in a reservoir rock (Baiyegunhi et al., 2017). Mechanical compaction (Fig. 10a-c) is generally thought to affect the actual loss of porosity in sandstone (Spencer, 1989; Sciscio, 2015; Li et al., 2021) while there have been two effects on porosity and permeability of reservoir with the influence of cementation. The porosity and permeability of the reservoir are reduced with cementing materials by filling intragranular and

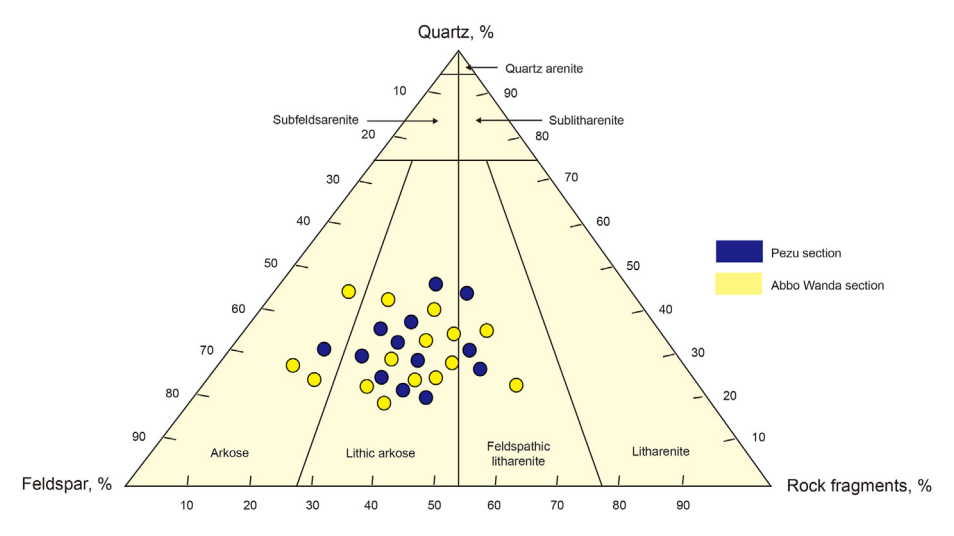


Fig. 7. The rock composition of Early Jurassic Datta sandstone. Ternary plot refers to the sandstone classification standard of Folk et al. (1970).

Table 1The petrographic composition of different microfacies.

Sr. No.	Microfacies	No. of Slides	Percentage, %
1	Arkosic sandstone microfacies	09	18
2	Lithic Arkosic sandstone microfacies	27	54
3	Feldspathic litharenite sandstone microfacies	11	22
4	Hybrid sandstone microfacies	03	06

intergranular pores (Fig. 10). The porosity and permeability of the reservoir up to a certain extent are improved by dissolution (Bjørlykke et al., 1989).

Datta Formation consists of primary intergranular pores (Fig. 13a and b) and secondary diagenetic pores (Fig. 13c-f), that have been examined through the thin section and scanning electron microscope analysis. The primary pores are intergranular pores (Fig. 13a and b), which depend on the maturity of the clasts, largely restricted by depositional events. While the secondary pores are intragranular secondary pores, dissolved pores, and fractured pores (Fig. 13c-f). The burial and thermal history suggest continuous and rapid subsidence and deposition developed during the burial. The studied formation is exposed in the studied area, but the buried sandstone is buried more than 3000 m depth and the average geothermal gradient is near 100 °C (Khalid et al., 2014). At that temperature, source rock becomes slightly mature, and pore volume reduces due to compaction and cementation, whereas due to fracturing and dissolution pores are developed that enhance the rock characteristics.

5. Discussion

5.1. Impact of diagenesis on reservoir quality

The sandstone experienced several diagenetic changes during the burial process and has a considerable impact on the porosity and permeability of reservoir rock in which the effect of cementation, compaction, and dissolution are the most noteworthy. The detrital grain dissolution and the protection of pore spaces due to the coating of clay mineral grain are the significant diageneses (constructive), while the compaction and the cementation development are the destructive diageneses (Lin et al., 2017). The important aspects in evaluating the quality of the reservoir are porosity and permeability, dependent on depositional controls like

grain sorting and grain size, detrital minerals, and diagenetic controls such as the formation of authigenic clay minerals, compaction, cementation, and dissolution (Islam, 2009; Schmid et al., 2004; Taylor et al., 2010; Kashif et al., 2018).

The analyzed samples of both sections had moderate to high compaction (Fig. 10a, c). Most of the grains exhibited point-contact to line-contact. Because of little conflict to compression and imposed pressure, and fracturing of brittle and weak minerals, the actual porosity is decreased (Paxton et al., 2023; Kashif et al., 2018) and leading to the flow of grains, and weak grains have been elastically deformed (Fig. 10b). Compaction decreases the pore volume and reduces the reservoir characteristics. Due to high burial, the compaction rate is also high and it can reduce the reservoir fluid accumulation space.

Blocking of the pores and pore throats through cementing materials including carbonates, silica, and clay minerals decreases the quality of the reservoir (Fig. 10; Fig. 13). Sandston comprises dominantly quartz and feldspar (Fig. 15), with good primary porosity. Clogging of primary pores, as well as secondary pores by clay minerals, reduces the reservoir characteristics. The porosity and permeability of the reservoir are decreased by calcite cement. The value of porosity and permeability are generally associated with distance from the sandstone—mudstone boundary. In general, sandstone units away from the sandstone/mudstone contact contain low content of carbonate cement and consisting high porosity and permeability values.

Quartz overgrowths cover the shape and roundedness of detrital grains under the microscope (Fig. 10b, d). Quartz overgrowth along the grain boundaries and within the pores decreases the reservoir characteristics (Figs. 8g, 9g and 11c and d; Fig. 12b). Generally, it decreases the pore volume, and also pore throat eliminates the storage capacity as well as fluid migration pathway. Most grains look sub-round and sub-angular in shape. The sediment shape depends upon the distance that sediment travels. Sediments

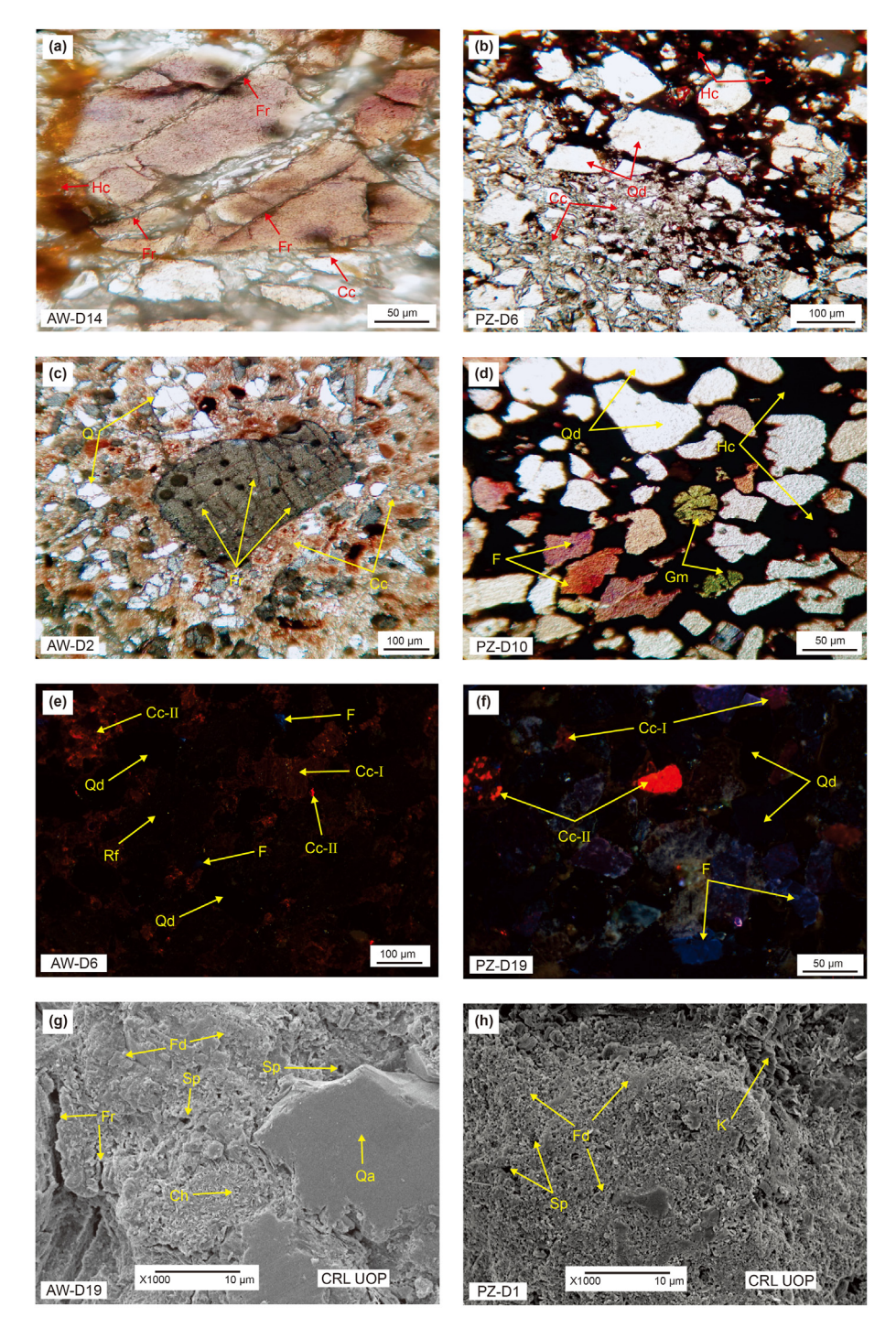


Fig. 8. Microphotographs of thin section, Cathodoluminescence (CL) and SEM show different digenetic processes in studied sections. (a) Calcite cement fills highly fractured grain, also cementation of grains by mostly calcite and hematite cement (AW-D14). (b) Cementation of grains by calcite (mostly) and hematite cement (AW-D10). (c) Highly fractured grains provide pathway for fluid flow, and cementation of grains by calcite (AW-D2). (d) Cementation of quartz and feldspar grains by hematite cement, glauconitic minerals (PZ-D14). (e) CL shows Early (older) stage Cc-I calcite cement and Later (younger) stage Cc-II calcite cement, and cement the rock fragments, quartz and feldspar grains (AW-D17), (f) Transformation of plagioclase (feldspar) into clay mineral chlorite, fractured and secondary pores (PZ-D1). (h) Transformation of plagioclase (feldspar) into clay mineral chlorite, fractured and secondary pores (PZ-D1). (h) Transformation of plagioclase (feldspar) into clay mineral kaolinite, secondary pores (AW-D19). Ppprimary pores, Sp-secondary pores, Fr-fractured pores, Fd-feldspar dissolution, Cc-I-Early-stage calcite cement, Cc-II-Later stage calcite cement, Hc-hematite cement, Fr-fractures, Gm-glauconitic minerals, Q-quartz, QA-authigenic quartz, F-feldspar, I/S-illite/smectite, Ch-chlorite, K-kaolinite.

containing more spherical grains have usually low porosity than sediments having fewer spherical grains. Quartz cement tends to reduce the porosity by considerably less than mechanical compaction and carbonate cement.

The effect of clay minerals on reservoir physical properties is generally attributed to the deposition of authigenic clay minerals blocking the pore space of the reservoir or reducing the connectivity of the reservoir (Wang et al., 2017). According to the X-ray

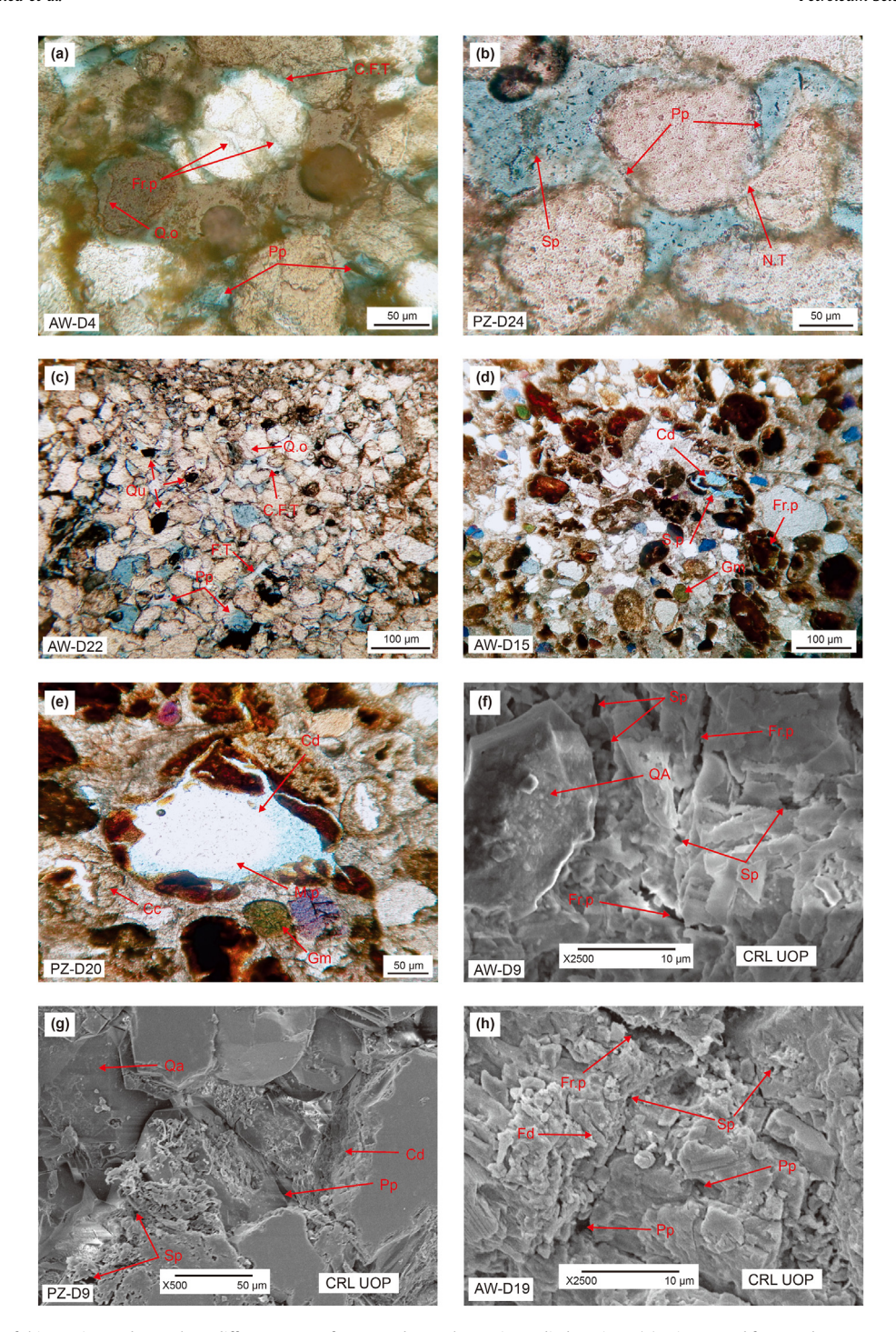


Fig. 9. Microphotographs of thin section and SEM show different types of pores and pore throats in studied sections. (a) Primary and fractured pores, curved flake pores throat (AW-D4). (b) Primary pores, secondary pores curved flake and neck pores throat(PZ-D24). (c) Primary pores and pores filled with oil, quartz overgrowth, curved flake, and flake pore throat (AW-D22). (d) Partial dissolution of feldspar result in the secondary pore, and fracture pore (AW-D15). (e) Wholly dissolution of grain results in moldic pore (PZ-D9). (f) Dissolution of feldspar results in the secondary pore, fracture pores and authigenic quartz (AW-D20). (g) Primary and secondary pores, authigenic quartz (PZ-D9). (h) Primary, secondary and fractured pores (AW-D19). Pp-primary pores, Sp-secondary pores, Fr.p-fractured pores, M.P-moldic pores, F.T-flake throat, N.F.T-neck flake throat, C.F.T-curved flake throat, Q.o-quartz overgrowth, Fd-feldspar dissolution, Qa-authigenic quartz.

diffraction results, kaolinite is the chief clay mineral, followed by mixed-layer illite/smectite, and chlorite (Fig. 14; Table 3; Table 4). Authigenic kaolinite often fills primary intergranular pores or feldspar dissolution pores with booklets-like or worm-like aggregates (Fig. 11a and b; Fig. 12c). Mixed layer illite/smectite was often in honeycomb form and was negatively correlated with porosity

and permeability, but their correlation with porosity was more optimized than that with permeability (Fig. 11a, f; Fig. 12a and b). The chlorite can restrain quartz overgrowth as well as preserve certain primary pores (Fig. 11d and e; Fig. 12d).

Dissolution of feldspar, authigenic clay precipitation, and the development of cement consisting of quartz and carbonate, are the

Table 2The core plug porosity and permeability values of selected samples of the Datta Formation.

S. No.	Lab Reference No.	Field Sample No.	Length, cm	Diameter, cm	Dry w.t., gm	Density, g/cc	Porosity, %	Permeability, mD
1	Pr.17297	PZ-D3c	5.39	2.53	67.54	2.79	13.23	0.86
2	Pr.17298	AW-D4c	2.79	2.42	26.06	2.65	26.89	149
3	Pr.17299	AW-D7c	2.47	2.45	26.02	2.70	20.24	115
4	Pr.17300	PZ-D15c	5.38	2.47	62.16	2.86	15.91	0.12
5	Pr.17301	AW-D9c	4.26	2.23	25.51	2.34	23.46	123
6	Pr.17302	PZ-D13c	4.63	2.43	26.01	2.29	20.07	114

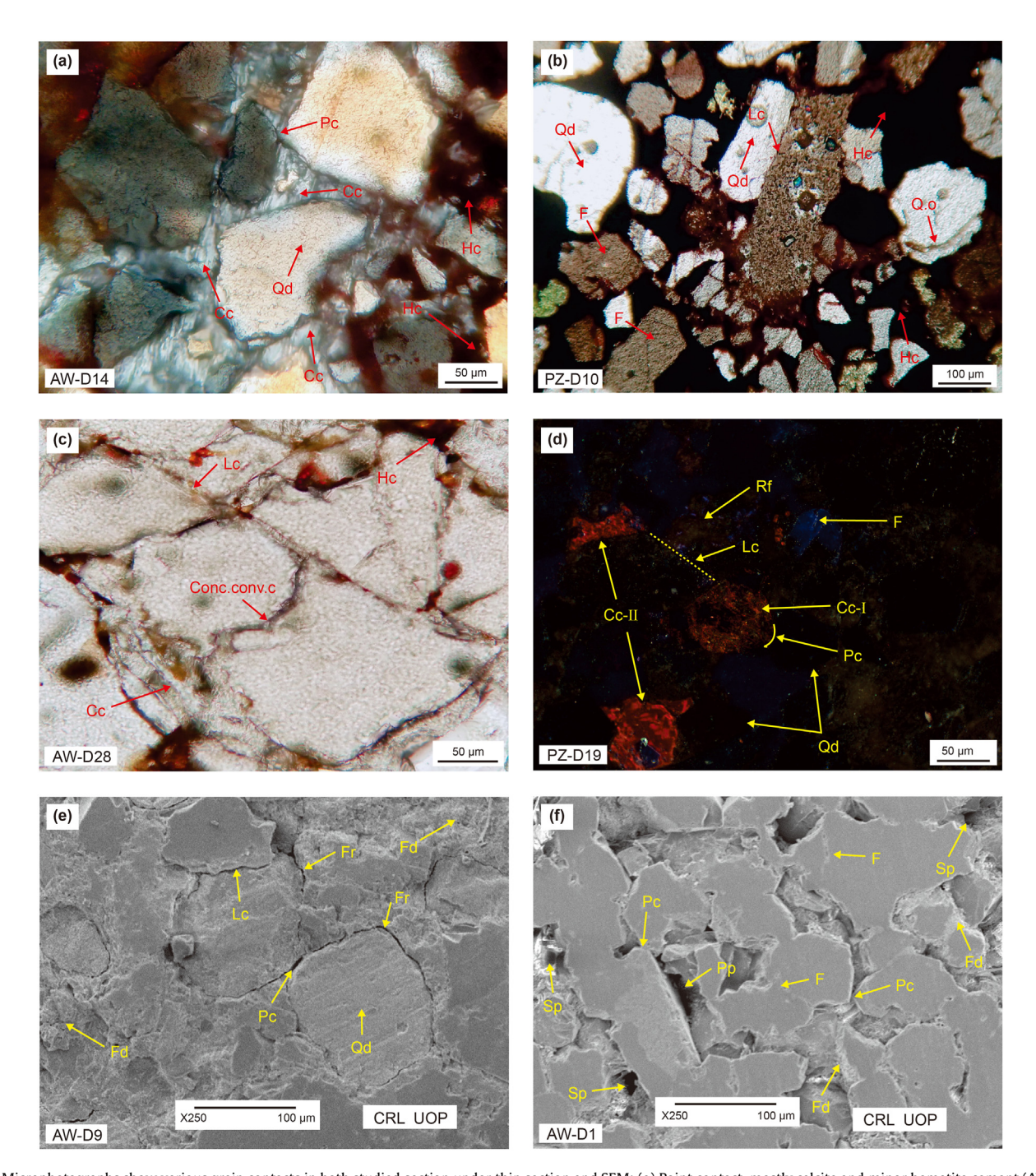


Fig. 10. Microphotographs show various grain contacts in both studied section under thin section and SEM; (a) Point contact, mostly calcite and minor hematite cement (AW-D14); (b) Line contact, quartz overgrowth, hematite act as cement (PZ-D10) (c) Concave-convex and line contact (AW-D28); (d)) CL shows Early stage (older) Cc-I and Later stage (younger) Cc-II calcite cement, and cement the rock fragments, quartz and feldspar grains, and line and point contacts among grains (PZ-D19); (e) Point and line contact and feldspar dissolution (AW-D9); (f) Point contact, Primary pores and feldspar dissolution creates secondary pores (AW-D1). Pc-point contact, Lc-line contact, Qd-detrital quartz, F-Feldspar, Fd-feldspar dissolution, Qo-quartz overgrowth, Hc-hematite cement, Cc-calcite cement, Pp-primary pores, Sp-secondary pores, C.c-I- Early-stage calcite cement, C.c-II-Later stage calcite cement.

M. Tariq, M. Kashif, N. Ahmed et al.

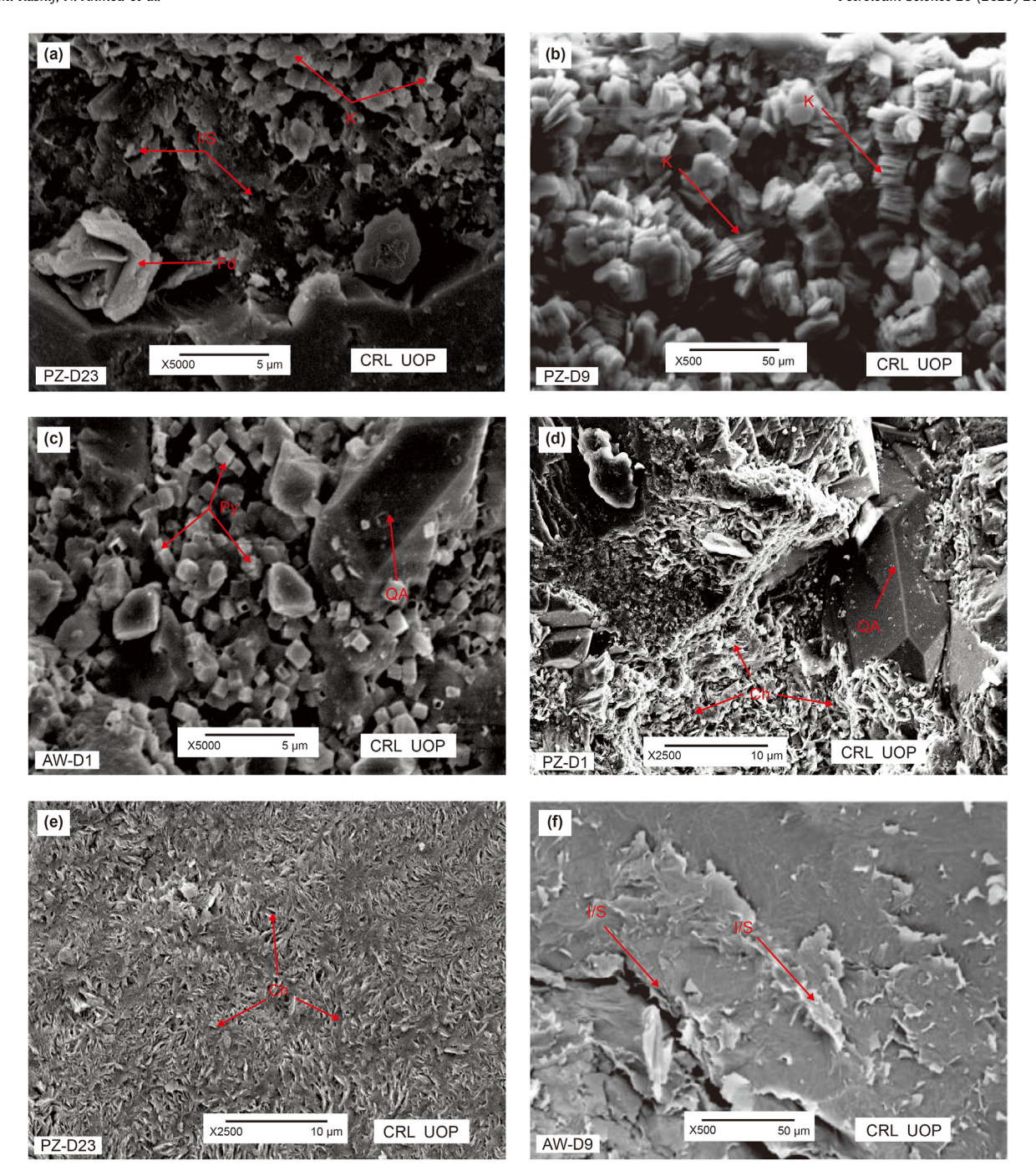


Fig. 11. Microphotographs show various clay minerals under SEM; (a) Illite/smectite clay, Feldspar dissolution, and authigenic quartz (PZ-D23); (b) Booklets of Kaolinite clay (PZ-D9); (c) The pyrite filling the intergranular pores (AW-D1); (d) Chlorite clay, Feldspar dissolution and authigenic quartz (PZ-D1); (e) Rosette-shape chlorite clay (PZ-D23); (f) Illite/smectite mixed-layer on the particle surface (AW-D9); I/S-illite/smectite, Ch-chlorite, K-kaolinite, QA-authigenic quartz.

chemical diagenetic processes that affect the sandstone's reservoir quality (Fig. 11). The substitution of K-feldspar by calcite/albite, change of plagioclase to illite, and feldspar dissolution are the changes in feldspar, which enhance the quality of the reservoir. Change of plagioclase into small grain size clay (Fig. 11; Fig. 12) with high content of organic matter is usually widespread in sandstone (Kashif et al., 2018, 2020). Grain-coating clay closely relates to primary porosity (Bloch et al., 2002; Ozkan et al., 2011). The greatest influence on reservoir physical properties was due to compaction, which reduces the reservoir quality while the greater

influence on reservoir chemical properties by fracturing and dissolution (Li et al., 2021), which enhances the reservoir quality.

Secondary porosity is created mainly by feldspars and unstable grain dissolution (Fig. 13). A large amount of intragranular and intergranular dissolution pores are developed at the meso-diagenetic stage through the dissolution of volcanic rock fragments and feldspar grains (Fig. 13). Overall compaction and cementation are the chief mechanisms that broadly reduce the reservoir's physical properties, while the dissolution process increases the porosity and permeability.

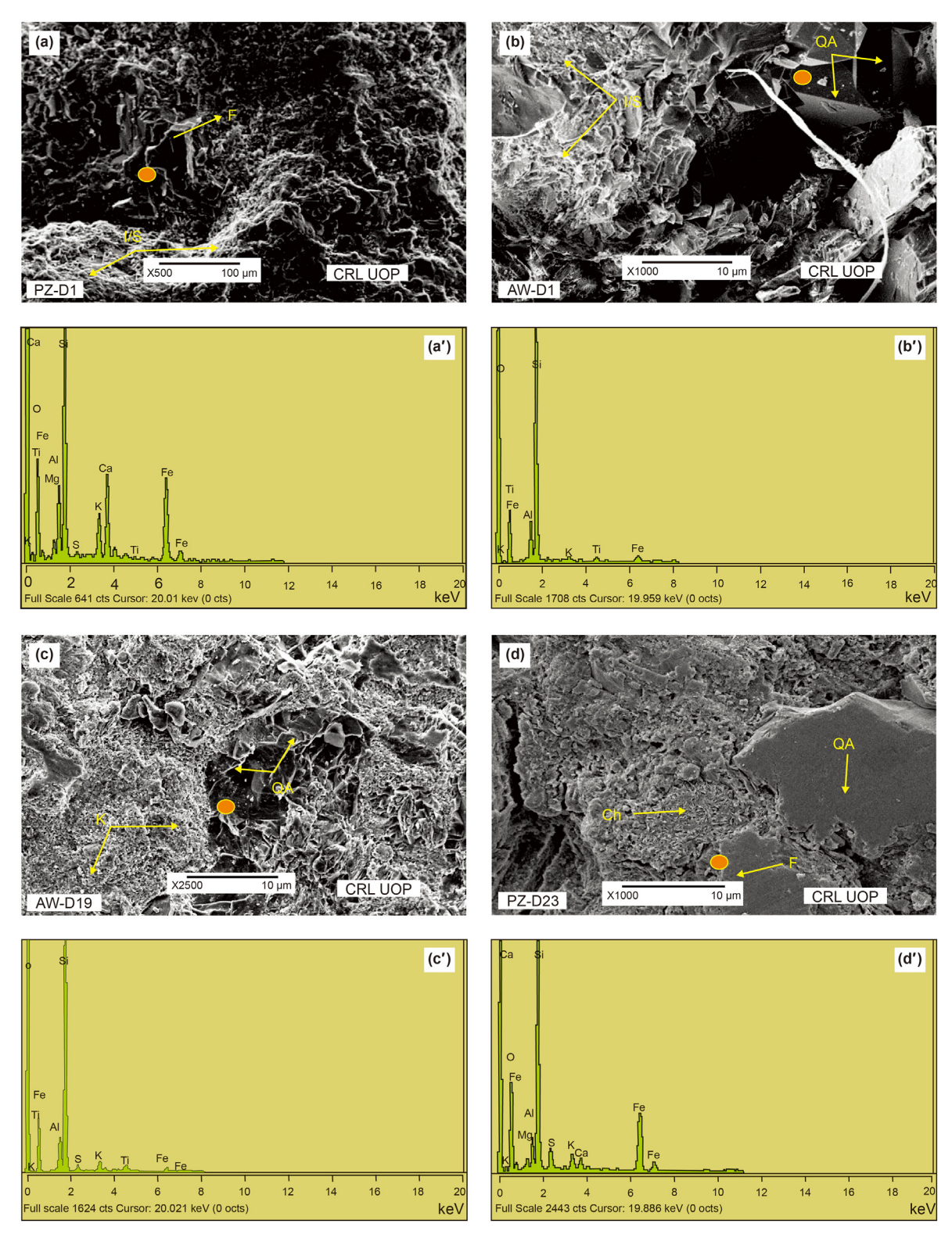


Fig. 12. Microphotographs of SEM and EDS of the marked site of both studies section shows clay mineral characteristics of Datta Formation; (a) Showing the honeycomb-shaped mixed-layer I/S between the pores (PZ-D1); (a') EDS graph shows that oxygen, silicon, iron and calcium are major element and other are minor elements which indicate that sample is mostly feldspar rich followed by quartz (PZ-D1); (b) Showing the honeycomb-shaped mixed-layer I/S between the pores (AW-D1); (b') EDS graph shows that oxygen and silicon are major element and other are minor elements which indicate that sample is mostly quartz rich (AW-D1); (c) Showing kaolinite between the pores (AW-D19); (c') EDS graph shows that oxygen and silicon are major element and other are minor elements which indicate that sample is mostly quartz rich (AW-D19); (d) Showing rosette- and needle-shaped chlorite (PZ-D23); (d') EDS graph shows that oxygen, silicon and iron are major element and other are minor elements which indicate that sample is mostly feldspar rich followed by quartz (PZ-D23). Qa,-authigenic quartz, K-kaolinite, I/S-mixed-layer illite/smectite, Ch-chlorite, F-feldspar.

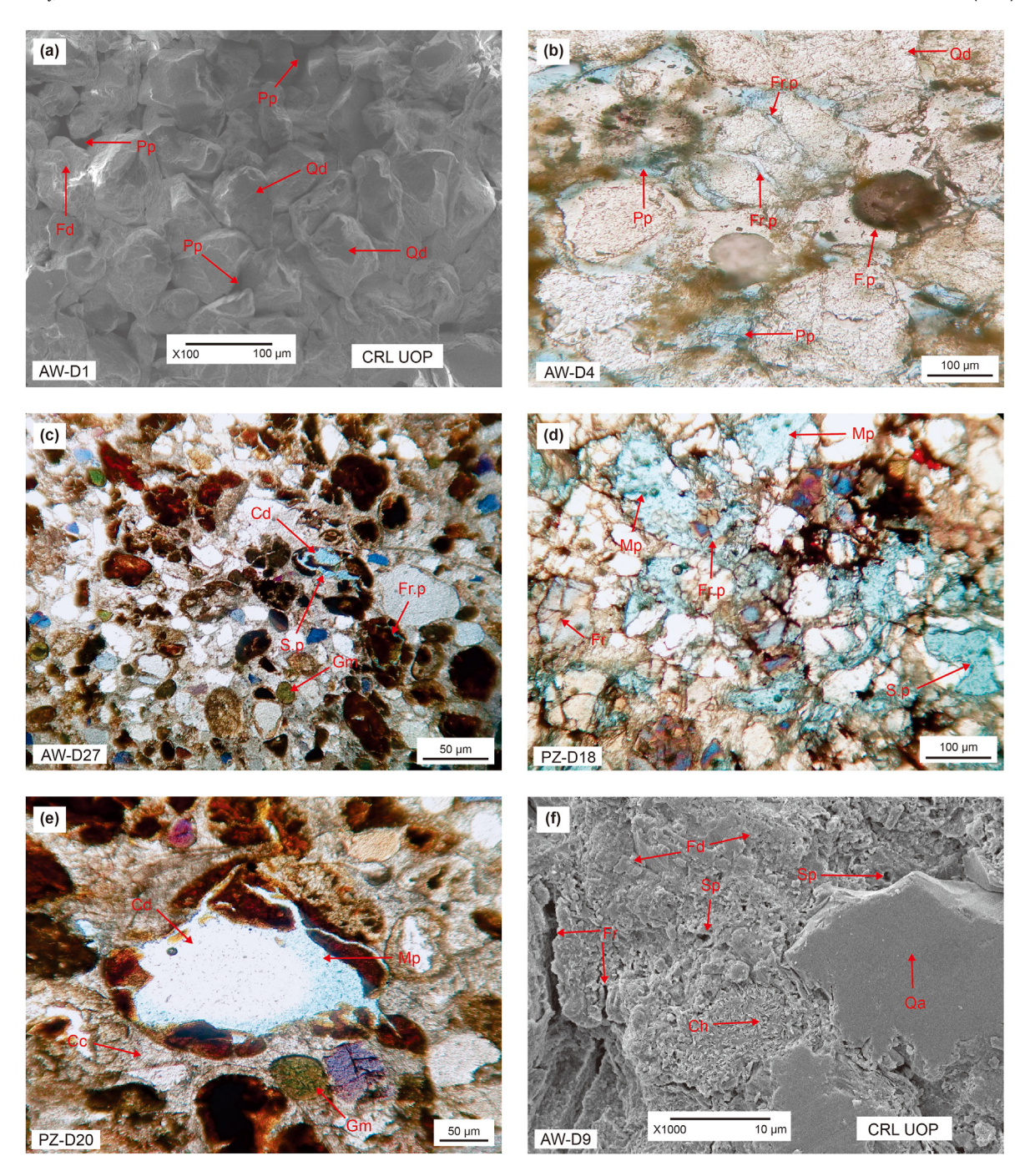


Fig. 13. SEM and thin section microphotographs show different types of pores in both studied sections. (a) Shows primary pores and detrital quartz (AW-D4). (b) Fractured and primary pores (AW-D27). (c) Dissolution of clasts creates secondary pores, and fracture pores (AW-D1). (d) Whole grain dissolution creates moldic pores, fractures and secondary pores (PA-D18). (e) Dissolution of whole clastic grain creates moldic pores (PZ-D20). (f) Shows feldspar dissolution creating secondary pores and altered into chlorite clay mineral, authigenic quartz, and fractures (AW-D9). Qd-detrital quartz, Qa-authigenic quartz, F-feldspar, Fd-feldspar dissolution, Cc-calcite cement, Pp-primary pores, Sp-secondary pores, Mp-moldic pores, Fr.p-fractured pores, Gm-glauconitic mineral, S.fr-secondary fractures, Ch-chlorite, F.p-fecal pellets.

5.2. Tectogenetic fracture effect on reservoir quality

Differential forces cause the uplift of the rock unit to expose to the surface of the earth. Fractures are created in siliciclastic as well as carbonate rocks due to tectonic activities. Tectonic activities made the Sheikh Badin Hills more complicated. The study area comprises normal faults that are followed by a sedimentary sequence thrusting which is south-directed over the basal decollement (Blisniuk et al.,

1998) resulting in a series of SW—NE oriented faults, and the fractures were developed. Fractures are generally formed during digenesis (during tectonic uplift) which causes the enhancement of the storage space as well as the migration pathway for fluids. In general, fractures increased the reservoir rock permeability, although the majority of fractures were partly or completely filled by other substances, due to which the contribution of fractures to the reservoir's development was restricted.

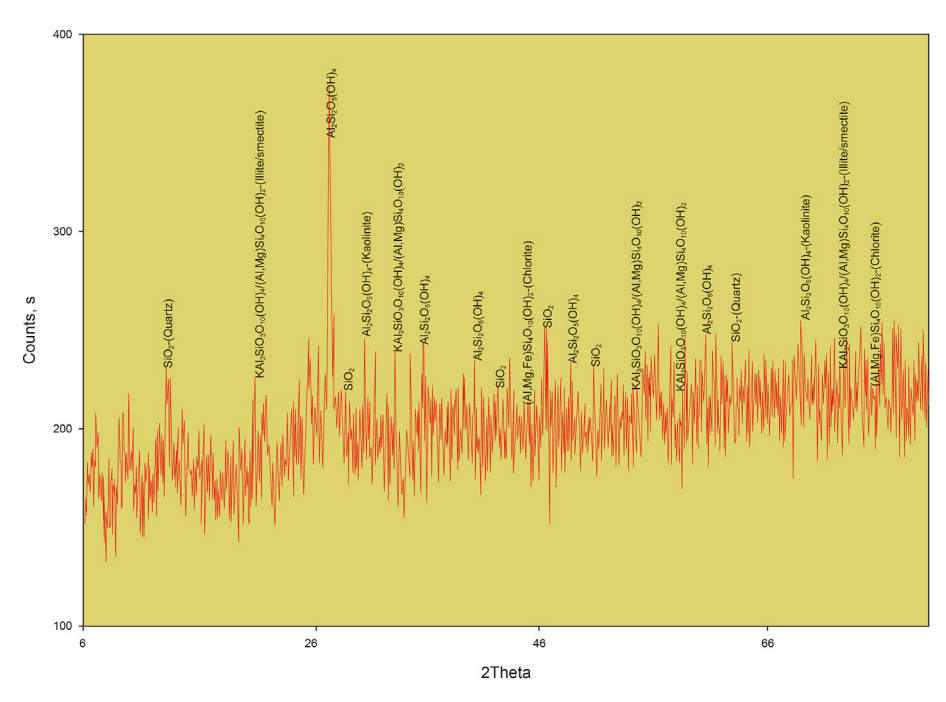


Fig. 14. A diffractogram of shale of the Datta Formation showing the peaks of kaolinite followed by mixed-layer illite/smectite, chlorite, and quartz.

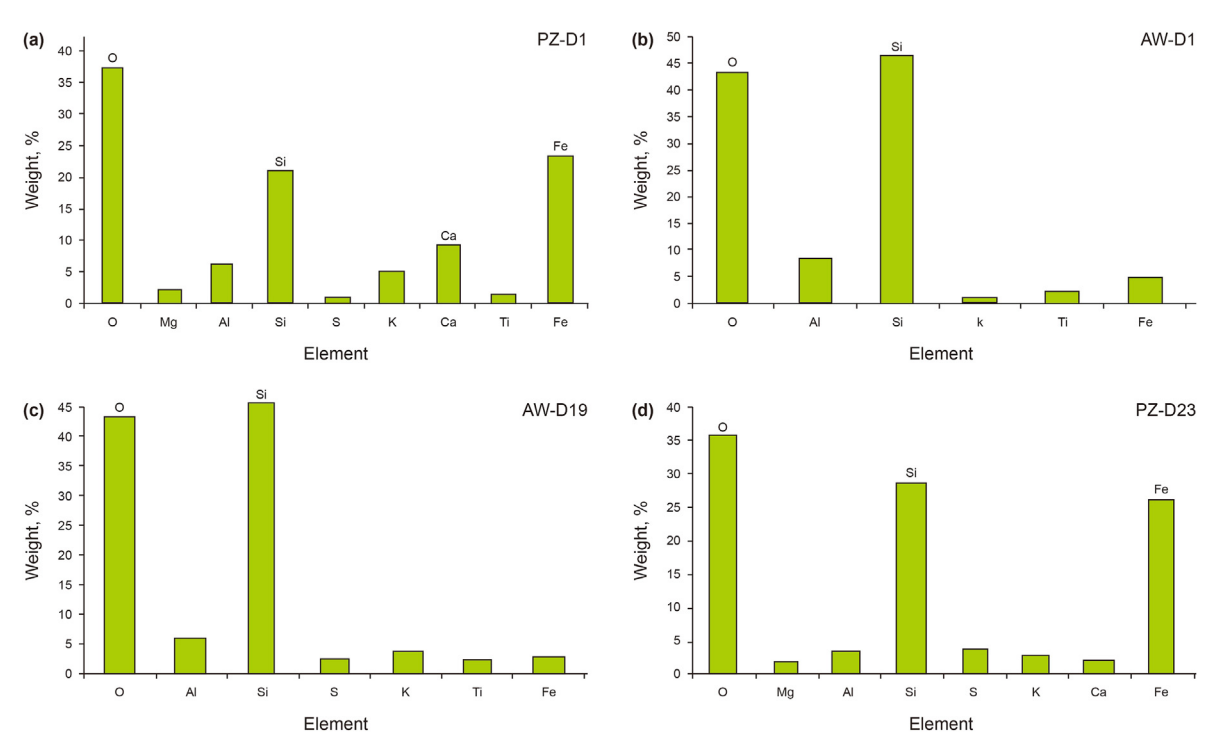


Fig. 15. A graphical representation of EDS elemental compositions of selected samples. (a) O oxygen, Si silicon, and Fe iron are the dominant, and other are minor elements, these indicate that the sample is mostly feldspar rich followed by quartz suggesting that the sample is mostly quartz-rich (PZ-D1) of Pezu section. (b) O oxygen and Si silicon are the dominant and others are minor elements (AW-D1) of Abbo Wanda section. (c) O oxygen and Si silicon are the dominant and others are minor elements which indicate that the sample is mostly quartz-rich (AW-D19) of Abbo Wanda section. (d) O oxygen, Si silicon, and Fe iron are the dominant, and others are minor elements which indicate that the sample is mostly feldspar rich followed by quartz (PZ-D23) of Pezu section.

Cracks and fractures are mainly caused by compaction and various tectonic stresses, which are beneficial to acidic or alkaline fluids permeating into particles, causing the dissolution of particles and the formation of dissolution fractures (Fig. 8a, c, g; Fig. 9a, d, f,

h; Fig. 11f). The existence of fractures allows for the further dissolution of unstable minerals and the enlargement of primary intergranular pores, which form the main channel and storage space for fluid migration, and they are crucial to the improvement of the

Table 3The elemental composition of the Pezu section (PZ-D1), oxygen, silicon, iron, and calcium are major elements and others are minor elements which indicate that the sample is mostly feldspar rich followed by quartz.

Element	Weight, %	Atomic, %
0	36.56	56.84
Al	5.43	5.01
Mg	1.74	1.78
Ti	0.67	0.35
Si	20.05	17.76
S	0.34	0.26
K	4.33	2.75
Ca	8.50	5.27
Fe	22.38	9.97
Total	100	100

Table 4The elemental composition of Abbo Wanda section (AW-D1), in which oxygen and silicon are major elements and others are minor elements indicating that the sample is mostly quartz-rich.

Element	Weight, %	Atomic, %
0	42.52	57.53
Al	5.00	4.01
Si	44.80	34.52
S	1.38	0.93
K	2.75	1.52
Ti	1.75	0.79
Fe	1.81	070
Total	100	100

physical properties of sandstone reservoirs (Chang et al., 2019; Lai et al., 2017). Generally, micro-fractures with openings which are greater than 0.1 μ m can become effective fractures for oil and gas migration (Yuan, 2011). Moreover, the fractures exhibited a good positive relationship with the core permeability, core porosity, and porosity of the thin section, and their correlation with permeability was more optimized than the porosity. The results show that the development of fractures can improve the reservoir space, and greatly improve the connectivity of pores, which play a significant role in enhancing the porosity and permeability of sandstone reservoirs.

5.3. Sedimentological impact on reservoir quality

Three main facies have been recognized including depositional facies based on depositional environment, lithofacies based on lithology, and microfacies based on petrographic analysis. The conglomeratic sandstone, coarse grain sandstone, and medium grain sandstones were generally deposited in the stream channel and lacustrine environment and fell in arkosic sandstone microfacies and lithic arkosic sandstone microfacies (Fig. 6; Fig. 7). As conglomeratic sandstone, coarse-grained sandstone and medium sandstone contain significant primary pores as well as the secondary dissolved pores, therefore acting as a good reservoir and enhancing the reservoir quality (Kashif et al., 2019) (Fig. 6; Fig. 9a-d, g; Fig. 13b-d). While siltstone and mudstone/shale were generally deposited in the floodplain and swampy environments with negligible primary pores and secondary pores with low permeability, therefore they have a negative impact on reservoir quality.

5.4. Reservoir quality by core plug porosity and permeability analyses

Porosity is expressed as a percentage of the volume of total rock and ranges from extremely low porosities (<1%) to very high (<45%). Both porosity and permeability remarkably depend on the pore's connectivity. Porosity is comprised of both primary and secondary dissolved pores (Fig. 8; Fig. 9), showing a range from <1% to 18.7% with an average of 9.78%. The intergranular primary porosity range from <1% to 15.60%, averaged as 8.40%, whereas the secondary dissolved porosity, derived from part or complete dissolution of unstable grain range from <1% to 4.50%.

The prominent predictable porosity and permeability of the Early Jurassic Datta Formation are further complemented by the quantitative core plug porosity and permeability analysis. Based on observation from standard core plug analysis of the core plug specimen of the Datta Formation, the core plug porosity and permeability values range from 13.23% to 26.89% with an average of 13%, and 0.12 to 149 mD with an average of 72 mD, respectively (Fig. 16; Table 2).

Some specimens have low permeability with high porosity, or high permeability with low porosity, and permeability is usually not related to the entire porosity, but it is generally controlled by pore network characteristics i.e pore and throat types, radius, and its combination. Overall the core plug porosity and thin section porosity, as well as core plug permeability, indicate that the studied Jurassic Datta sandstone may act as a reservoir for oil and gas exploration.

6. Conclusions

- (1) The outcrop examination allows the recognition of six lithofacies (conglomeratic sandstone, coarse-grain sandstone, medium-grain sandstone, fine-grain sandstone, siltstone, and mudstone/shale) with different sedimentary structures (lamination, load cast, cross-stratification, hummocky cross beddings, honeycomb structure, and biogenic structures). Three main microfacies i.e arkosic sandstone, lithic arkosic, and feldspathic litharenite sandstone microfacies have been established. The sedimentary structures and lithofacies point out that the Datta Formation was deposited in a deltaic environment. The conglomeratic sandstone, coarse sandstone, and medium sandstone have good primary and secondary porosity and permeability, therefore acting as a good reservoir. While the siltstone and mudstone/shale have very low primary and secondary porosity acting as low reservoir rock.
- (2) Sandstone consisting of moderate to high mechanical compaction, grains are mostly cemented by calcite followed by hematite and quartz overgrowth as a cement, and dissolution of unstable gains and feldspar and precipitation of clay minerals were important diagenetic features. Compaction and cementation reduced the reservoir quality whereas dissolution and fracturing enhance the reservoir quality.
- (3) Core plug porosity and permeability analysis describe the physical properties of reservoir rock, through the quality of reservoir rock can be evaluated. Core plug porosity and permeability as well as the total porosity of the thin section were positively correlated with the secondary dissolved pores. The core plug porosity and permeability range from 13.23% to 26.89% with an average of 13%, and 0.12 to 149 mD

S. No.	Lab Ref. No.	Field sample No.	Plug length, cm	Plug diameter, cm	Dry weight, gram	Grain density, g/cc	Porosity,	Permeability, mD	Field samples	Core plug
1	Pr.17297	PZ-D3c	5.39	2.53	67.54	2.79	13.23	0.86	PZ-D3c	Pr.17297
2	Pr.17298	AW-D4c	2.79	2.42	26.06	2.65	26.89	149	AW-D4c	Pr.17298
3	Pr.17299	AW-D7c	2.47	2.45	26.02	2.70	20.24	115	AW-D7c	Pr.17299
4	Pr.17300	PZ-D15c	5.38	2.47	62.16	2.86	15.91	0.12	PZ-D15c	Pr.17300
5	Pr.17301	AW-D9c	4.26	2.23	25.51	2.34	23.46	123	AW-D9c	Pr.17301
6	Pr.17302	PZ-D13c	4.63	2.43	26.01	2.29	20.07	114	PZ-D13c	Pr.17302

Fig. 16. The core plug porosity and permeability values of selected samples of the Datta Formation.

averaged as 72 mD, respectively. Based on the above observations and experiments, the Datta Formation in the studied area has good reservoir quality and great potential for hydrocarbon development and exploration.

Declaration of competing interest

All authors have read and approved the version of this manuscript, and due care has been taken to ensure the integrity of the work. It is not being submitted to any other journal. We believe this paper may be of particular interest to the readers of your journal.

Acknowledgment

The authors acknowledged the Department of Earth Sciences, University of Sargodha, Sargodha to provide the basic facilities, as well as acknowledged the Center of the Excellence, University of Peshawar, Pakistan for providing experimental facilities. We are also thankful to the editor, and the anonymous reviewers, for their constructive comments to improve the manuscript. This research work was funded by ourselves.

References

Alam, I., 2008. Stratigraphic and Structural Framework of the Marwat-Khisor Ranges, NWFP, Pakistan. Ph.D Thesis. National Centre of Excellence in Geology, University of Peshawar, Pakistan, pp. 1–142. http://173.208.131.244:9060/ xmlui/handle/123456789/3525.

Baiyegunhi, C., Liu, K., Gwavava, O., 2017. Diagenesis and reservoir properties of the permian ecca group sandstones and mudrocks in the eastern cape province, South Africa. Minerals 7 (6), 88. https://doi.org/10.3390/min7060088.

Bjørlykke, K., Ramm, M., Saigal, G.C., 1989. Sandstone diagenesis and porosity modification during basin evolution. Geol. Rundsch. 78 (1), 243–268. https:// doi.org/10.1007/BF01988363.

Blisniuk, P.M., Sonder, L.J., Lillie, R.J., 1998. Foreland normal fault control on northwest Himalayan thrust front development. Tectonics 17 (5), 766–779. https://doi.org/10.1029/98TC01870.

Bloch, S., Lander, R.H., Bonnell, L., 2002. Anomalously high porosity and permeability in deeply buried sandstone reservoir: origin and predictability. Am. Assoc. Petrol. Geosci.Bull. 86, 301–328. https://doi.org/10.1306/61EEDABC-173E-11D7-8645000102C1865D.

Bosence, D.W., Nichols, G., Al Subbary, A., AL Thour, K.A., Reader, M., 1996. Syn-rift continental to marine depositional sequences, tertiary Gulf of Aden. Yemen,J. Sediment Res. 66, 766–777. https://doi.org/10.1306/D4268400-2B26-11D7-8648000102C1865D.

Brannin, J., Sahota, Gurdip, Gerdes, K.D., Berry, J.A.L., 1999. Geological evolution of the central Marib—Shabwah basin. Yemen. GeoArabia. 4, 9—34. https://doi.org/10.2113/geoarabia040109.

Chang, X., Wang, Y., Shi, B., Xu, Y., 2019. Charging of carboniferous volcanic

- reservoirs in the eastern Chepaizi uplift, Junggar Basin (northwestern China) constrained by oil geochemistry and fluid inclusion. Am. Assoc. Petrol. Geol. Bull. 103, 1625–1652. https://doi.org/10.1306/12171818041.
- Chester, J.S., Lenz, S.C., Chester, F.M., Lang, R.A., 2004. Mechanisms of compaction of quartz sand at diagenetic conditions. Earth Planet Sci. Lett. 220 (3–4), 435–451. https://doi.org/10.1016/S0012-821X(04)00054-8.
- Csato, I., Habib, A., Kiss, K., Kocz, I., Kovacs, V., Lorincz, K., Milota, K., 2001. Play concepts of oil exploration in Yemen. Oil Gas J. 99, 68–74.
- Fatmi, A.N., Kennedy, W.J., 1999. Maastrichtian ammonites from balochistan, Pakistan. J. Paleontol. 73 (4), 641–662. https://doi.org/10.1017/S0022336000032467.
- Folk, R.L., Andrews, P.B., Lewis, D., 1970. Detrital sedimentary rock classification and nomenclature for use in New Zealand. N. Z. J. Geol. Geophys. 13, 937–968. https://doi.org/10.1080/00288306.1970.10418211.
- Gee, E.R., 1989. Overview of the Geology and structure of the Salt Range, with observations on related areas of northern Pakistan. GSA (Geol. Soc. Am.) Spec. Pap. (Reg. Stud.) 232, 95–112. https://doi.org/10.1130/SPE232-p95.
- Hakimi, M.H., Shalaby, M., Abdullah, W.H., 2012. Diagenetic characteristics and reservoir quality of the Lower Cretaceous Biyadh sandstones at Kharir oilfield in the western central Masila basin, Yemen. J. Asian Earth Sci. 51, 109–120. https:// doi.org/10.1016/j.jseaes.2012.03.004.
- Hammer, E., Mørk, M.B.E., Naess, A., 2010. Facies controls on the distribution of diagenesis and compaction in fluvial-deltaic deposits. Mar. Petrol. Geol. 27 (8), 1737–1751. https://doi.org/10.1016/j.marpetgeo.2009.11.002.
- Hemphill, W.R., Kidwai, A.H., 1973. Stratigraphy of Bannu and Dera Ismail Khan Area, Pakistan. United States Geological Survey, Professional Papers, pp. 1–36. https://doi.org/10.3133/pp716B, 716- B.
- Islam, A.M., 2009. Diagenesis and reservoir quality of bhuban sandstones (neogene), titas gas field, bengal basin, Bangladesh. J. Asian Earth Sci. 35, 89–100. https:// doi.org/10.1016/i.iseaes.2009.01.006.
- Kashif, M., Cao, Y., Yuan, G., Asif, M., Jian, W., Zhukhun, W., Naz, A.F., 2019. Sedimentological impact on reservoir quality of Es1 sandstone of Shahejie formation, Nanpu Sag, East China. Arabian J. Geosci. 12 (17), 1–21. https://doi.org/10.1007/s12517-019-4671-y.
- Kashif, M., Cao, Y., Yuan, G., Asif, M., Rehman, F., Shehza, K., Mustafa, G., 2020. Sedimentology of shahejie formation, bohai bay basin: a case study of E s 1 member in nanpu sag. Carbonates Evaporites 35, 1–18. https://doi.org/10.1007/ s13146-020-00579-4
- Kashif, M., Cao, Y., Yuan, G., Jian, W., Cheng, X., Sun, P., Hassan, S., 2018. Diagenesis impact on a deeply buried sandstone reservoir (Es1 member) of the shahejie formation, nanpu sag, bohai bay basin, east China. Aust. J. Earth Sci. 66 (1), 133–151. https://doi.org/10.1080/08120099.2018.1490357.
- Kazmi, A.H., Rana, R.A., 1982. Tectonic Map of Pakistan 1:2000000: Map Showing Structural Features and Tectonic Stages in Pakistan. Geological Survey of
- Khalid, P., Naeem, M., Haroon, A.M., Din, Z.U., Yasin, Q., 2014. Petroleum play analysis, structural and stratigraphic interpretation of cretaceous sequence, Punjab Platform, central Indus Basin, Pakistan. Sci. Int. 26 (5), 2163–2171. https://doi.org/10.1007/s12594-014-0183-2.
- Lai, J., Wang, G.W., Fan, Z.Y., Wang, Z.Y., Chen, J., Zhou, Z.L., Wang, S.C., Xiao, C.W., 2017. Fracture detection in oil-based drilling mud using a combination of borehole image and sonic logs. Mar. Petrol. Geol. 84, 195–214. https://doi.org/ 10.1016/j.marpetgeo.2017.03.035.
- Li, W., Fan, T., Gao, Z., Wu, Z., Li, Y.N., Zhang, X., Cao, F., 2021. Impact of diagenesis on the low permeability sandstone reservoir: case study of the lower jurassic

- reservoir in the niudong area, northern margin of qaidam basin. Minerals 11 (5), 453. https://doi.org/10.3390/min11050453.
- Lin, W., Chen, L., Lu, Y., Hu, H., Liu, L., Liu, X., Wei, W., 2017. Diagenesis and its impact on reservoir quality for the Chang 8 oil group tight sandstone of the Yanchang Formation (upper Triassic) in southwestern Ordos basin, China. J. Pet. Explor. Prod. Technol. 7 (4), 947–959. https://doi.org/10.1007/s13202-017-0340-4.
- Miall, A.D., 2013. Principles of Sedimentary Basin Analysis, third ed. Springer Science & Business Media New York. https://doi.org/10.1007/978-3-662-03999-1.
- Ozkan, A., Cumella, S.P., Milliken, K.L., Laubach, S.E., 2011. Prediction of lithofacies and reservoir quality using well logs, late cretaceous williams fork formation, mamm creek field, piceance basin, Colorado. Am. Assoc. Petrol. Geosci..Bull. 95, 1699–1723. https://doi.org/10.1306/01191109143.
- Paxton, S.T., Szabo, J.O., Ajdukiewicz, J.M., Klimentidis, R.E., 2023. Construction of an intergranular volume compaction curve for evaluating and predicting compaction and porosity loss in rigid-grains sandstone reservoir. Am. Assoc. Petrol.Geol. Bull. 86. https://doi.org/10.1306/61EEDDFA-173E-11D7-8645000102C1865D.
- Pettijohn, F., Potter, P., Siever, R., 2012. Sand and Sandstone, second ed. Springer Science & Business Media, Berlin. https://doi.org/10.1007/978-1-4612-1066-5.
- Schmid, S., Worden, R.H., Fisher, Q.J., 2004. Diagenesis and reservoir quality of the sherwood sandstone (triassic), corrib field, slyne basin, west of Ireland. Mar. Petrol. Geol. 21, 299–315. https://doi.org/10.1016/j.marpetgeo.2003.11.015.
- Sciscio, L., 2015. Position of the Triassic-Jurassic Boundary in South Africa and Lesotho: A Multidisciplinary Approach Aimed at Improving the Chronostratigraphy and Biostratigraphy of the Elliot Formation, Stormberg Group. PhD thesis. University of Cape Town, South Africa, p. 301. http://hdl.handle.net/ 11477/20847
- Spencer, C.W., 1989. Review of characteristics of low-permeability gas-reservoirs in western United States. Am. Assoc. Petrol. Geosci.,Bull. 73, 613–629. https:// archives.datapages.com/data/bulletns/1988-89/data/pg/0073/0005/0600/0613. htm
- Taylor, T.R., Giles, M.R., Hathon, L.A., Diggs, T.N., Braunsdorf, N.R., Birbiglia, G.V., 2010. Sandstone diagenesis and reservoir quality prediction: models, myths, and reality. Am. Assoc. Petrol. Geosci..Bull. 94, 1093–1132. https://doi.org/ 10.1306/04211009123.
- Tucker, M., 1988. Techniques in Sedimentology||. Blackwell Scientific Publications, Oxford, London, pp. 1–394. UK. https://agris.fao.org/agris-search/search.do?recordID=US201300619538
- Wang, L., Tian, Y., Yu, X., Wang, C., Yao, B., Wang, S., Wu, Y.S., 2017. Advances in improved/enhanced oil recovery technologies for tight and shale reservoirs. Fuel 210, 425–445. https://doi.org/10.1016/j.fuel.2017.08.095.
- Yu, X., Li, S., Li, S., 2018. Clastic Hydrocarbon Reservoir Sedimentology. Springer. https://doi.org/10.1007/978-3-319-70335-0.
- Yaseen, M., Wahid, S., Ahmad, S., Rehman, G., Ahmad, J., Anjum, M.N., Mehmood, M., 2021. Tectonic evolution, prospectivity and structural studies of the hanging wall of Main Boundary Thrust along Akhurwal-Kohat transect, Khyber Pakhunkhwa: implications for future exploration. Arabian J. Geosci. 14, 1–17. https://doi.org/10.1007/s12517-021-06651-0.
- Yuan, Z., 2011. Study on the Characteristics and Control. Factors Analysis of Oil & Gas. Reservoir of the Upper Triassic in Southeast. Ordos Basin. Northwestern University, Xi'an, China.
- Zaidi, S.N.A., Brohi, I.A., Ramzan, K., Ahmed, N., Mehmood, F., Brohi, A.U., 2013. Distribution and hydrocarbon potential of Datta sand in upper Indus Basin Pakistan. Sindh Univ. J. -SURJ (Sci. Series) 45 (2).